

Unified Data Management and Comprehensive Performance Evaluation for Urban Spatial-Temporal Prediction [Experiment, Analysis & Benchmark]

Jiawei Jiang
jwjiang@buaa.edu.cn

School of Computer Science and Engineering, Beihang University
Beijing, China

Wayne Xin Zhao
batmanfly@gmail.com

Gaoling School of Artificial Intelligence, Renmin University of China
Beijing, China

Chengkai Han
ckhan@buaa.edu.cn

School of Computer Science and Engineering, Beihang University
Beijing, China

Jingyuan Wang*
jywang@buaa.edu.cn

School of Computer Science and Engineering, School of Economics and Management, Beihang University
Beijing, China

ABSTRACT

The field of urban spatial-temporal prediction is advancing rapidly with the development of deep learning techniques and the availability of large-scale datasets. However, challenges persist in accessing and utilizing diverse urban spatial-temporal datasets from different sources and stored in different formats, as well as determining effective model structures and components with the proliferation of deep learning models. This work addresses these challenges and provides three significant contributions. Firstly, we introduce "atomic files", a unified storage format designed for urban spatial-temporal big data, and validate its effectiveness on 40 diverse datasets, simplifying data management. Secondly, we present a comprehensive overview of technological advances in urban spatial-temporal prediction models, guiding the development of robust models. Thirdly, we conduct extensive experiments using diverse models and datasets, establishing a performance leaderboard and identifying promising research directions. Overall, this work effectively manages urban spatial-temporal data, guides future efforts, and facilitates the development of accurate and efficient urban spatial-temporal prediction models. It can potentially make long-term contributions to urban spatial-temporal data management and prediction, ultimately leading to improved urban living standards.

PVLDB Reference Format:

Jiawei Jiang, Chengkai Han, Wayne Xin Zhao, and Jingyuan Wang. Unified Data Management and Comprehensive Performance Evaluation for Urban Spatial-Temporal Prediction [Experiment, Analysis & Benchmark]. PVLDB, 14(1): XXX-XXX, 2020.
doi:XX.XX/XXX.XX

PVLDB Artifact Availability:

*Corresponding author

This work is licensed under the Creative Commons BY-NC-ND 4.0 International License. Visit <https://creativecommons.org/licenses/by-nc-nd/4.0/> to view a copy of this license. For any use beyond those covered by this license, obtain permission by emailing info@vldb.org. Copyright is held by the owner/author(s). Publication rights licensed to the VLDB Endowment.

Proceedings of the VLDB Endowment, Vol. 14, No. 1 ISSN 2150-8097.
doi:XX.XX/XXX.XX

The source code, data, and/or other artifacts have been made available at <https://github.com/LibCity>.

1 INTRODUCTION

In recent years, the advancements in sensor technology in urban areas have facilitated the collection of a vast amount of urban spatial-temporal data. This data offers new perspectives for leveraging artificial intelligence technologies to address urban spatial-temporal prediction challenges [65]. Urban spatial-temporal prediction plays a crucial role in urban computing, enabling efficient management and decision-making in smart cities. Various applications benefit from urban spatial-temporal prediction, including congestion control [15], route planning [30], vehicle dispatching [77], and POI recommendation [69].

The fundamental distinction between urban spatial-temporal data and conventional time-series data lies in that spatial-temporal data comprises historical state time series from multiple spatial entities that exhibit mutual influences. Consequently, the spatial-temporal prediction problem can be formulated as a multivariate time series prediction problem [6, 54] rather than a univariate time series prediction problem [24]. Effectively modeling the spatial relationships among the time series of different entities stands as the key to solving the spatial-temporal prediction problem.

Traditional time series forecasting methods, such as VAR [21] and ARIMA [53], fail to consider the spatial dependencies inherent in urban spatial-temporal data. In contrast, deep learning methods exhibit superior feature learning capabilities and are more effective in capturing spatial-temporal correlations. Consequently, numerous deep learning-based urban traffic prediction techniques have been proposed in the literature. Initially, researchers utilized convolutional neural networks (CNNs) to model spatial dependencies within Euclidean neighborhoods. This approach represented cities as grids, with CNNs employed to capture relationships among the time series of grid cells. As research advanced, the focus shifted towards modeling relationships between time series observed across different variables using a graph structure. Graph convolutional networks (GCNs) emerged as a popular choice for capturing spatial

dependence in urban spatial-temporal data. Learning graph structures [78] has become a mainstream approach in spatial-temporal prediction, and spatial attention mechanisms have also been explored to capture the dynamic graph structures among variables.

The field of urban spatial-temporal prediction is experiencing rapid advancements driven by the development of deep learning techniques and the availability of large-scale datasets. However, several challenges still need to be addressed: Firstly, accessing and utilizing existing urban spatial-temporal datasets can be challenging due to their diverse sources and formats. These datasets are often stored in different formats, such as NPZ, PKL, H5, CSV, and soon. This heterogeneity creates barriers for users to effectively utilize and explore the datasets, particularly for newcomers in the field. This hinders the development and standardization of the field and presents obstacles to efficient data management and utilization.

Secondly, with the proliferation of deep learning models in the domain, it becomes increasingly difficult to determine effective model structures and designs. Deep learning models have demonstrated state-of-the-art performance in spatial-temporal prediction, leading to a surge in research papers in this area. However, as models become more complex and diverse, it is challenging to identify which techniques are truly effective and which directions hold potential for future research. The sensitivity of deep learning models to experimental parameters and configurations further emphasizes the need to explore valuable research directions and identify the most promising approaches. To address the challenges above, we make the following contributions in this paper:

(1) **Unified Storage Format:** We introduce a unified storage format called "atomic files" specifically designed for urban spatial-temporal big data. Through the validation of 40 diverse datasets, we demonstrate the effectiveness of this format in simplifying the management of urban spatial-temporal data. This contribution addresses the challenge of accessing and utilizing diverse datasets stored in different formats, enables accurate and efficient urban prediction, and enhances related applications.

(2) **Technical Development Roadmap:** We present a comprehensive overview of the technological advances in urban spatial-temporal prediction models. This roadmap outlines techniques for effectively modeling spatial dependencies, temporal dependencies, and spatial-temporal fusion using deep learning. By providing this roadmap, we facilitate the development of advanced and robust urban spatial-temporal prediction models, empowering researchers to fully leverage the potential of deep learning in this domain.

(3) **Extensive Experiments and Performance Evaluation:** We conduct extensive experiments using 18 models and 20 datasets, establishing a performance leaderboard and comparing previous works in spatial-temporal prediction. Through these experiments, we gain valuable insights into model performance and identify promising directions for future research. This evaluation enables researchers and practitioners to make informed decisions and drive advancements in urban spatial-temporal prediction.

By introducing the atomic files storage format, providing a technical roadmap, and conducting comprehensive experiments, we contribute to effectively managing urban spatial-temporal data, guiding future research efforts, and facilitating the development of accurate and efficient urban spatial-temporal prediction models. These contributions aim to address the challenges faced by the

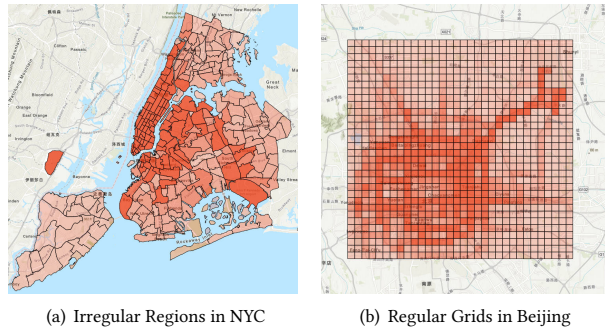


Figure 1: Different division methods of plane-based data.

field and accelerate progress in urban spatial-temporal prediction, ultimately improving the quality of urban living.

The subsequent sections are organized as follows: Section 2 introduces the unified storage format for spatial-temporal data. Section 3 presents the problem formalization of urban spatial-temporal prediction. Section 4 outlines the development roadmap for deep models in urban spatial-temporal prediction. Section 5 describes the comprehensive experiments conducted to compare different models and gain insights. Section 6 provides the conclusion.

2 UNIFIED SPATIAL-TEMPORAL DATA MANAGEMENT

With the rapid progress of technology, a large amount of urban spatial-temporal data has been accumulated, offering fresh insights for addressing urban traffic prediction challenges. Common urban spatial-temporal data include traffic state data, trajectory data, meteorological data, air quality data, etc. Nevertheless, these spatial-temporal data often exist in various formats, posing additional obstacles for researchers aiming to harness the full potential of such data. In this section, we present a unified storage format designed specifically for urban spatial-temporal big data and demonstrate its efficacy through validation using 40 diverse datasets. We firmly believe that this format will significantly simplify the management of urban spatial-temporal data.

2.1 Spatial-Temporal Data Unit

In this section, we analyze the basic units underlying the urban spatial-temporal data.

2.1.1 Basic Unit. The most basic unit in spatial-temporal data is the geographical unit. According to the difference in spatial distribution, the basic geographical unit data are divided into three types:

(1) **Point-based Data:** This type of data mainly includes urban point of interest (POI) data, GPS sampling points, urban traffic sensors, traffic cameras, and other device data. We can use (geo_i, l_i, p_i) to represent the point data, where geo_i is the ID of this point, l_i is the location of the point i , such as latitude and longitude information, and p_i is the attribute information of the point i , such as the POI category.

(2) **Line-based Data:** This type of data is mainly the road segment data. Similarly, we can use (geo_i, l_i, p_i) to represent the line-based data, where geo_i is the ID of the road segment, l_i is the location of the road segment, which usually includes the latitude

and longitude of the starting and ending locations, and \mathbf{p}_i is the attributes of road segment i , such as the average speed.

(3) **Plane-based Data:** This type of data is mainly urban region data such as administrative districts. In particular, the city grid data obtained by the grid division of the city area is also plane-based data. The different methods of dividing the city area are given in Figure 1. Similarly, we can use $(geo_i, l_i, \mathbf{p}_i)$ to represent the plane-based data, where geo_i is the ID of the region, l_i is the location of this region, which usually includes the latitude and longitude of the regional boundary locations, and \mathbf{p}_i is the attribute information of region i , such as the traffic inflow or outflow of the region.

2.1.2 Unit Relations. The unit relation data describes the relationships between geographical units in urban space, e.g., road connectivity and distance relationships. Given that these relationships exhibit diverse structures, we further refine the interconnections between geographical units in the following manner:

(1) **Graph Relation Data:** Graph network data includes urban sensor graph, POI graph, road network graph, region graph, and soon. In general, we can define such graph data as $\mathcal{G} = (\mathcal{V}, \mathcal{E}, F_{\mathcal{V}}, \mathbf{A})$, where \mathcal{V} is a set of N nodes ($N = |\mathcal{V}|$), $\mathcal{E} \subseteq \mathcal{V} \times \mathcal{V}$ is a set of edges, $F_{\mathcal{V}} \in \mathbb{R}^{N \times D}$ is a D -dimension attribute matrix, and $\mathbf{A} \in \mathbb{R}^{N \times N}$ is a weighted adjacency matrix between nodes.

(2) **Grid Relation Data:** A common Euclidean neighborhood data is the city grid data, which can be represented as $F_{\mathcal{V}} \in \mathbb{R}^{I \times J \times D}$, where the city is divided into $I \times J$ grids, and each grid $V^{(i,j)}$ has D attributes. Each grid matches the distribution of the surrounding grids in the Euclidean neighborhood.

(3) **Graph OD Relation Data:** This kind of data focuses on the relation between the origin and the destination, which is a more fine-grained relational data. We use $F_{\mathcal{E}} \in \mathbb{R}^{N \times N \times D}$ to denote the D -dimension OD data between each pair of nodes in \mathcal{V} (or say the D -dimension data of each edge), where each entry $F_{\mathcal{E}}^{(i,j)} \in \mathbb{R}^D$ represents D -dimension attributes from node v_i to node v_j .

(4) **Grid OD Relation Data:** In particular, for the OD data between city grids, it can be denoted by $F_{\mathcal{E}} \in \mathbb{R}^{I \times J \times I \times J \times D}$, and each entry $F_{\mathcal{E}}^{(i_1, j_1), (i_2, j_2)}$ represents D -dimension attributes from $Grid^{(i_1, j_1)}$ to $Grid^{(i_2, j_2)}$.

Let us clarify the difference between Graph Relation Data and Graph OD Relation Data. Graph Relation Data pertains to the attributes of the graph nodes, i.e., $F_{\mathcal{V}} \in \mathbb{R}^{N \times D}$, such as the traffic speed of each node, in a graph network \mathcal{G} . On the other hand, Graph OD Relation Data is concerned with the attributes of the graph edges, i.e., $F_{\mathcal{E}} \in \mathbb{R}^{N \times N \times D}$, which represents the transfer flow from the start to the end of the edge. This is typically used to model traffic flow between origin-destination pairs in transportation networks. Similarly, for Grid Relation Data, we can refine it into OD data between each pair of grids, where the attributes of the edges represent the traffic flow between the grids.

2.1.3 Unit Dynamics. Spatial-temporal dynamic data refers to the attribute information of city geographical units that change over time. We can obtain complex spatial-temporal data by incorporating dynamic attributes in the temporal dimension into the unit relation data. Examples of such data include urban traffic flow,

Table 1: Symbols for Unit Relations and Unit Dynamics

Types	Unit Relations	Unit Dynamics
Graph Relation Data	$F_{\mathcal{V}} \in \mathbb{R}^{N \times D}$	$\mathbf{X} \in \mathbb{R}^{T \times N \times D}$
Grid Relation Data	$F_{\mathcal{V}} \in \mathbb{R}^{I \times J \times D}$	$\mathbf{X} \in \mathbb{R}^{T \times I \times J \times D}$
Graph OD Relation Data	$F_{\mathcal{E}} \in \mathbb{R}^{N \times N \times D}$	$\mathbf{X} \in \mathbb{R}^{T \times N \times N \times D}$
Grid OD Relation Data	$F_{\mathcal{E}} \in \mathbb{R}^{I \times J \times I \times J \times D}$	$\mathbf{X} \in \mathbb{R}^{T \times I \times J \times I \times J \times D}$

traffic speed, and ridership demand, all exhibiting dynamic spatial-temporal characteristics. To illustrate this, let's consider graph relation data. When the graph attribute $F_{\mathcal{V}} \in \mathbb{R}^{N \times D}$ changes over time, we can represent the D -dimensional spatial-temporal attributes of N nodes at T time slices using a spatial-temporal tensor denoted as $\mathbf{X} \in \mathbb{R}^{T \times N \times D}$. To comprehensively understand different data types, please refer to Table 1 to explore the intuitive relationship between unit relations and unit dynamics.

2.1.4 External Information. External data refers to environmental information that provides additional context related to spatial-temporal dynamics. These data sources offer auxiliary information that can enhance the accuracy of urban spatial-temporal predictions. Examples of external data include city traffic accidents, major events, and calendar data, which encompass factors such as the day of the week, time of day, and the presence of holidays. By incorporating these external sources, we can leverage their valuable insights to improve the precision of spatial-temporal predictions.

2.2 Atomic files

Existing open-source spatial-temporal datasets are often stored in various formats. This situation inevitably creates challenges and burdens for users who wish to utilize these datasets. To address this issue, based on the analysis of spatial-temporal data units, relations, and dynamics discussed in the previous section, we propose the concept of "atomic files" as a solution, which offers a unified storage and management format for urban spatial-temporal data. These atomic files represent the minimum information units of urban spatial-temporal data. They can be classified into four types: Geographical Unit Data, Unit Relation Data, Spatial-temporal Dynamic Data, and External Data (Optional).

We adopt a comma-separated value format, similar to the CSV file, for storing the four types of atomic files. Each atomic file comprises multiple columns of data. To differentiate between different types of atomic files, we assign specific file suffixes. Additionally, we enforce specific guidelines for the information contained in each line of the atomic files, as outlined in Table 2. The precise definitions are as follows:

(1) The ".geo" tables store the Geographical Unit Data, which are required to include `geo_id` (the primary key), geographic unit type (point, line, or polygon), and coordinate information (such as longitude and latitude). Other additional properties should be stored after the three columns above, such as the category of the point of interests (POIs) or the length of the road segments.

(2) The ".rel" tables store the Unit Relation Data, which should consist of `rel_id` (the primary key), `origin_id`, and `des_id`. The `origin_id` and `des_id` represent the IDs of the origin and destination entities in the relationship, respectively. These IDs are derived from

Table 2: Summary of Atomic Files

Suffix	Content	Format
.geo	Geographical Unit Data	geo_id, type, coordinates, [properties]
.rel	Unit Relation Data	rel_id, origin_id, des_id, [properties]
.dyna	Graph Relation Dynamic Data	dyna_id, time, entity_id, [properties]
.grid	Grid Relation Dynamic Data	dyna_id, time, row_id, col_id, [properties]
.od	Graph OD Relation Dynamic Data	dyna_id, time, origin_id, des_id, [properties]
.gridod	Grid OD Relation Dynamic Data	dyna_id, time, origin_row_id, origin_col_id, des_row_id, des_col_id, [properties]
.ext	External Information	ext_id, time, [properties]

the geo_id column (the foreign key) in the ".geo" table. Optionally, other properties can be included to indicate the weight of the relationship. Each row in the ".rel" table represents a directed edge from the origin to the destination.

(3) The Spatial-temporal Dynamic Data is stored in the ".dyna", ".grid", ".od", and ".gridod" tables, which are further divided into four sub-files due to the different unit relations. Each row in these tables represents an attribute of a geographic entity (or entity relationship) collected at a specific time. For instance, the dyna table stores spatial-temporal dynamic data related to graph relation data. It is required to include dyna_id (the primary key), time, entity_id, and at least one attribute, such as air quality and traffic flow. The time column represents the timestamp of the data collection, and the entity_id column indicates the source of data collection. The main distinction among these four types of tables lies in the entity_id column. In the dyna table, the entity_id is derived from the geo_id. In the grid table, the entity_id is derived from a grid's row and column ID corresponding to the geo_id for simplicity. In the ".od" table, the entity_id represents the origin_id and des_id of the OD relation entity. Lastly, in the ".gridod" table, the entity_id corresponds to the row and column ID of a grid OD relation entity.

(4) The ".ext" tables store the External Data, which must contain ext_id (the primary key), time, and at least one attribute.

To facilitate comprehension, we present an example of the Los Angeles traffic speed dataset in Figure 2. This dataset comprises three atomic files: geo, rel, and dyna, as it does not include any corresponding external data. Notably, the origin_id column, des_id column within the ".rel" table, and the entity_id column within the ".dyna" table are derived from the geo_id column in the ".geo" table. Specifically, the ".geo" table contains the locations of 207 road sensors. The ".rel" table stores the distance relationships between these sensors, commonly used to construct graph structures. Lastly, the ".dyna" table records the average traffic speed information collected by these sensors at 5-minute intervals from March to June 2012.

To validate the effectiveness of the atomic file format, we gathered 40 spatial-temporal dynamic datasets from 17 cities and transformed them into the atomic file format as presented in Table 3. The processed datasets, along with the associated data conversion scripts, are available at GitHub¹. We firmly believe that employing a unified data storage format can significantly alleviate the challenges associated with managing the urban spatial-temporal data. This standardization will enable more individuals to utilize urban spatial-temporal data and propel the rapid advancement of the urban spatial-temporal data field.

¹<https://github.com/LibCity/Bigcity-LibCity-Datasets>

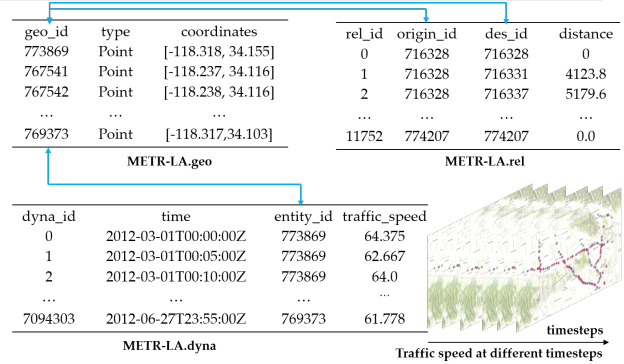


Figure 2: Example of atomic files: METR-LA dataset.

3 PROBLEM FORMALIZATION

The objective of urban spatial-temporal prediction tasks is to forecast future attributes based on historical observations of urban spatial-temporal data. The prediction tasks encompass various domains, such as traffic state prediction (e.g., flow, speed), on-demand service prediction, air quality prediction, climate prediction (e.g., wind speed, temperature), crime frequency prediction [52].

In a formal sense, let us consider the urban spatial-temporal dynamic data X as defined in Section 2.1.3. This problem aims to learn a mapping function f that utilizes the previous T time steps' observation values to predict the attributes of future T' time steps [47, 51, 63]. The urban spatial-temporal prediction problem can be formulated as follows:

$$[X(t - T + 1), \dots, X(t); \mathcal{G}] \xrightarrow{f} [X(t + 1), \dots, X(t + T')]. \quad (1)$$

4 ROADMAP FOR SPATIAL-TEMPORAL PREDICTION MODELS

In this section, we present an overview of the technical development roadmap for urban spatial-temporal prediction models. The urban spatial-temporal prediction task aims to make forecasts by capturing the spatial-temporal dependencies in spatial and temporal data. Traditional statistical methods and machine learning techniques, such as VAR [21], ARIMA [53], and SVR [12], rely on linear time-series analysis and fall short in effectively capturing spatial-temporal dependencies. However, the emergence of deep

²<https://www1.nyc.gov/site/tlc/about/tlc-trip-record-data.page>

³<https://www.kaggle.com/c/pkdd-15-predict-taxi-service-trajectory-i>

⁴<https://www.citibikenyc.com/system-data>

⁵<https://data.world/ride-austin/ride-austin-june-6-april-13>

⁶<https://www.capitalbikeshare.com/system-data>

⁷<https://www.divvybikes.com/system-data>

Table 3: Summary of Processed Urban Spatial-temporal Dynamic Datasets

DATASET	#GEO	#REL	#DYNA	PLACE	DURATION	#TS	DATA TYPE
METR-LA [32]	207	11,753	7,094,304	Los Angeles, USA	Mar. 1, 2012 - Jun. 27, 2012	5min	Graph Speed
Los-Loop [75]	207	42,849	7,094,304	Los Angeles, USA	Mar. 1, 2012 - Jun. 27, 2012	5min	Graph Speed
SZ-Taxi [75]	156	24,336	464,256	Shenzhen, China	Jan. 1, 2015 - Jan. 31, 2015	15min	Graph Speed
Q-Traffic [33]	45,148	63,422	264,386,688	Beijing, China	Apr. 1, 2017 - May 31, 2017	15min	Graph Speed
Loop Seattle [7, 8]	323	104,329	33,953,760	Greater Seattle Area, USA	Jan. 1, 2015 - Dec. 31, 2015	5min	Graph Speed
PEMSD7(M) [66]	228	51,984	2,889,216	California, USA	Weekdays of May. Jun., 2012	5min	Graph Speed
PEMS-BAY [32]	325	8,358	16,937,700	San Francisco Bay Area, USA	Jan. 1, 2017 - Jun. 30, 2017	5min	Graph Speed
Rotterdam [20]	208	-	4,813,536	Rotterdam, Holland	135 days of 2018	2min	Graph Speed
PEMSD3 [45]	358	547	9,382,464	California, USA	Sept. 1, 2018 - Nov. 30, 2018	5min	Graph Flow
PEMSD7 [45]	883	866	24,921,792	California, USA	Jul. 1, 2016 - Aug. 31, 2016	5min	Graph Flow
Beijing subway [70]	276	76,176	248,400	Beijing, China	Feb. 29, 2016 - Apr. 3, 2016	30min	Graph Flow
M-dense [9]	30	-	525,600	Madrid, Spain	Jan. 1, 2018 - Dec. 21, 2019	60min	Graph Flow
SHMetro [36]	288	82,944	1,934,208	Shanghai, China	Jul. 1, 2016 - Sept. 30, 2016	15min	Graph Flow
HZMetro [36]	80	6,400	146,000	Hangzhou, China	Jan. 1, 2019 - Jan. 25, 2019	15min	Graph Flow
NYCTaxi-Dyna ²	263	69,169	574,392	New York, USA	Jan. 1, 2020 - Mar. 31, 2020	60min	Region Flow
PEMSD4 [18]	307	340	5,216,544	San Francisco Bay Area, USA	Jan. 1, 2018 - Feb. 28, 2018	5min	Graph Flow, Speed, Occupancy
PEMSD8 [18]	170	277	3,035,520	San Bernardino Area, USA	Jul. 1, 2016 - Aug. 31, 2016	5min	Graph Flow, Speed, Occupancy
TaxiBJ2013 [72]	32*32	-	4,964,352	Beijing, China	Jul. 1, 2013 - Oct. 30, 2013	30min	Grid In&Out Flow
TaxiBJ2014 [72]	32*32	-	4,472,832	Beijing, China	Mar. 1, 2014 - Jun. 30, 2014	30min	Grid In&Out Flow
TaxiBJ2015 [72]	32*32	-	5,652,480	Beijing, China	Mar. 1, 2015 - Jun. 30, 2015	30min	Grid In&Out Flow
TaxiBJ2016 [72]	32*32	-	6,782,976	Beijing, China	Nov. 1, 2015 - Apr. 10, 2016	30min	Grid In&Out Flow
T-Drive [67, 68]	32*32	-	3,686,400	Beijing, China	Feb. 1, 2015 - Jun. 30, 2015	60min	Grid In&Out Flow
Porto ³	20*10	-	441,600	Porto, Portugal	Jul. 1, 2013 - Sept. 30, 2013	60min	Grid In&Out Flow
NYCTaxi140103 ²	10*20	-	432,000	New York, USA	Jan. 1, 2014 - Mar. 31, 2014	60min	Grid In&Out Flow
NYCTaxi140112 [38]	15*5	-	1,314,000	New York, USA	Jan. 1, 2014 - Dec. 31, 2014	30min	Grid In&Out Flow
NYCTaxi150103 [59]	10*20	-	576,000	New York, USA	Jan. 1, 2015 - Mar. 1, 2015	30min	Grid In&Out Flow
NYCTaxi160102 [34]	16*12	-	552,960	New York, USA	Jan. 1, 2016 - Feb. 29, 2016	30min	Grid In&Out Flow
NYCBike140409 [72]	16*8	-	562,176	New York, USA	Apr. 1, 2014 - Sept. 30, 2014	60min	Grid In&Out Flow
NYCBike160708 [59]	10*20	-	576,000	New York, USA	Jul. 1, 2016 - Aug. 29, 2016	30min	Grid In&Out Flow
NYCBike160809 [34]	14*8	-	322,560	New York, USA	Aug. 1, 2016 - Sept. 29, 2016	30min	Grid In&Out Flow
NYCBike200709 ⁴	10*20	-	441,600	New York, USA	Jul. 1, 2020 - Sept. 30, 2020	60min	Grid In&Out Flow
AustinRide ⁵	16*8	-	282,624	Austin, USA	Jul. 1, 2016 - Sept. 30, 2016	60min	Grid In&Out Flow
BikeDC ⁶	16*8	-	282,624	Washington, USA	Jul. 1, 2020 - Sept. 30, 2020	60min	Grid In&Out Flow
BikeCHI ⁷	15*18	-	596,160	Chicago, USA	Jul. 1, 2020 - Sept. 30, 2020	60min	Grid In&Out Flow
NYCTaxi-OD ²	263	69,169	150,995,927	New York, USA	Apr. 1, 2020 - Jun. 30, 2020	60min	OD Flow
NYC-TOD [37]	15*5	-	98,550,000	New York, USA	Jan. 1, 2014 - Dec. 31, 2014	30min	Grid-OD Flow
NYCTaxi150103 [59]	10*20	-	115,200,000	New York, USA	Jan. 1, 2015 - Mar. 1, 2015	30min	Grid-OD Flow
NYCBike160708 [59]	10*20	-	115,200,000	New York, USA	Jul. 1, 2016 - Aug. 29, 2016	30min	Grid-OD Flow
NYC-Risk [49]	243	59,049	3,504,000	New York, USA	Jan. 1, 2013 - Dec. 31, 2013	60min	Risk
CHI-Risk [49]	243	59,049	3,504,000	New York, USA	Jan. 1, 2013 - Dec. 31, 2013	60min	Risk

learning has opened up new possibilities for researchers to harness its potential in urban spatial-temporal prediction. Deep learning methods offer the ability to fully exploit the spatial-temporal dependencies in the data. The subsequent section presents a comprehensive summary of techniques for modeling spatial dependencies, temporal dependencies and fusing spatial-temporal information, which serves as the foundation for our experiments.

4.1 Spatial Dependencies

Spatial dependencies are present in urban spatial-temporal data, as per the first law of geography, that "everything is related to everything else, but things that are close to each other are more closely related." Moreover, due to the division of urban structural and functional areas, urban spatial-temporal data has a spatial hierarchy. Therefore, even distant locations may exhibit strong spatial dependencies due to the similarity of functions. The spatial dependencies in data are the core difference between spatial-temporal prediction tasks and the time series prediction tasks.

(1) **Convolutional Neural Networks (CNNs)**: CNNs are widely used for modeling Grid Relation Data as these data are Euclidean data. Researchers often divide cities into grids based on latitude and longitude, which allows the spatial-temporal attribute data to be viewed as images. In this way, CNNs can extract spatial dependencies from different grids [34, 38, 50, 60]. For instance, ST-ResNet [72] utilizes a deep residual CNN network for traffic flow prediction.

(2) **Graph Neural Networks (GNNs)**: GNNs are widely used for modeling Graph Relation Data due to their strong ability to represent graphs [2–4, 6, 11, 14, 22, 23, 26, 27, 32, 35, 41, 44, 45, 55, 62, 66, 73–75]. Among GNNs, graph convolutional neural networks (GCNs)[10] are the most commonly used for spatial-temporal prediction tasks. An essential issue in graph convolution models is the construction of the graph adjacency matrix, and early studies typically used static adjacency matrices [32, 66]. However, predefined graph adjacency matrices may not accurately reflect the actual spatial dependencies in spatial-temporal data. To address this, adaptive graph generation modules have been proposed [2, 56]. Additionally, some studies have focused on learning dynamic spatial dependencies to model the effects of changes in the data over time [19, 22, 73]. To model continuous spatial dependencies, Graph ODE-based models have been used for spatial-temporal prediction [13].

(3) **Spatial Attention Mechanisms**: The spatial attention mechanism plays an essential role in modeling time-varying spatial dependencies between geographical entities [18, 19, 29, 38, 39, 57, 58, 64, 71, 76]. Through the spatial attention, models can autonomously learn the dynamic spatial dependencies embedded in the spatial-temporal data by assigning adaptive weights to different locations at different time steps. For instance, GMAN [76] proposes both spatial and temporal attention mechanisms and designs a gated fusion to fuse spatial and temporal information. ASTGNN [19] introduces a dynamic graph convolution module with a self-attention mechanism to capture spatial dependencies in a dynamic graph.

4.2 Temporal Dependencies

Urban spatial-temporal data displays temporal dependencies, similar to time-series data, which exhibit characteristics such as closeness, periodicity, and trend. For example, a traffic jam at 8

am can impact the traffic situation at 9 am, and rush hours tend to occur at similar times on consecutive workdays following a 24-hour cycle. Furthermore, holidays and weekdays can also have distinct effects on urban spatial-temporal data patterns.

(1) **Recurrent Neural Networks (RNNs)**: RNNs are a type of neural network designed to process sequential data and are thus well-suited for capturing the temporal dependencies in spatial-temporal data [2, 7, 14, 32, 38, 58, 60, 62, 75]. To address the RNNs' inability to model long-term dependencies, LSTM [25] and GRU [5] are introduced as variants of the original RNN model. These models incorporate a gating mechanism that allows them to capture longer-term dependencies. The Seq2Seq model [46] is a popular framework that uses RNNs as both encoders and decoders to enable multi-step spatial-temporal prediction.

(2) **Temporal Convolutional Networks (TCNs)**: TCNs are designed to process sequential data in a parallel fashion, which is impossible with Recurrent Neural Networks (RNNs) due to their reliance on historical information. TCNs are essentially 1-D CNN models that are used in the field of time series forecasting. They consider only the information before a given time step and are called causal convolutions. To increase the receptive field, dilated convolutions are used with causal convolutions. Multiple layers of dilated causal convolutions (also known as WaveNet [48]) can be stacked to achieve exponential growth of the receptive field. TCNs / 1D-CNN have become a common infrastructure in the field of spatial-temporal prediction [16–18, 39, 55, 56, 66].

(3) **Temporal Attention Mechanisms**: The temporal attention mechanism enables adaptive learning of nonlinear temporal dependencies in spatial-temporal data by assigning different weights to data at different time steps [1, 16, 18, 29, 34, 39, 57, 76]. This mechanism helps address the limitation of RNN models in modeling long-term dependencies, especially when combined with the Seq2Seq model. Recently, self-attention-based Transformer models have shown promising results in time series forecasting and have been applied to urban spatial-temporal prediction. For example, PDFormer [29] introduces a spatial-temporal self-attention mechanism to urban traffic flow prediction and incorporates the time-delay property of traffic state propagation.

4.3 Spatial-Temporal Dependencies Fusion

To capture the spatial-temporal dependencies in data, it is common to combine spatial and temporal models into a hybrid model, such as CNN+RNN, GCN+RNN, GCN+TCN, etc. The following are some common methods for fusing spatial and temporal models:

(1) **Sequential Structure**: The sequential structure combines the spatial and temporal neural networks in either parallel or serial configurations to form a spatial-temporal block [7, 18, 43, 55–57, 66, 75, 76]. For example, STGCN [66] utilizes 2 TCNs and 1 GCN to create a spatial-temporal block and stack them serially to capture the spatial-temporal dependencies in the data. TGCN [75] adopts a recursive approach by combining GCNs and GRUs, processing the input data recursively with GRUs after passing through GCNs at each time step. PDFormer [29] employs multiple spatial self-attention heads and temporal self-attention heads to learn the spatial-temporal dependencies in the data.

(2) **Coupled Structure**: The coupled structure integrates spatial neural networks into the computation of temporal neural networks, most commonly by combining GCNs and RNNs [2, 3, 32, 62]. In this approach, the fully connected operations in the computation of RNNs, including variants like GRU and LSTM models, are replaced with GCN operations. By doing so, the models can incorporate spatial dependencies into the learning of temporal dependencies. Some examples of this approach include DCRNN [32], CCRNN [62], MRABGCN [3], and AGCRN [2], etc.

(3) **Spatial-Temporal Synchronized Learning**: Previous research on modeling spatial-temporal dependencies in data has often used separate components to independently learn spatial and temporal dependencies. However, a spatial-temporal synchronous learning approach can simultaneously directly capture local spatial-temporal dependencies in the data. To accomplish this, a spatial-temporal local graph structure is constructed across time steps, and GCN is used to learn spatial-temporal dependencies. STSGCN [45] and STFGCN [31] are two examples of this approach.

5 EXPERIMENTS

In this section, we perform extensive experiments using diverse models and datasets with the aim of establishing a performance leaderboard. Our objective is to compare previous works in the field of spatial-temporal prediction and identify noteworthy directions for future research. Through these experiments, we seek to provide valuable insights and recommendations.

5.1 Datasets

In this section, we consider a total of 20 datasets, categorized into two types: Graph Relation Data and Grid Relation Data. The datasets we use are as follows. New datasets released in this study do not have any citations followed, while others with citations are open-sourced datasets. Please refer to Table 3 for more details.

(1) **Graph Relation Data**: These datasets consist of traffic speed or flow data recorded by traffic sensors. The following datasets are considered: METR-LA [32], PEMS-BAY [32], PEMS7(M) [66], PEMS3 [18], PEMS4-Speed [18], PEMS8-Speed [18], PEMS4-Flow [18], PEMS8-Flow [18], PEMS4-Occupy [18], and PEMS8-Occupy [18].

(2) **Grid Relation Data**: These datasets consist of city grid traffic inflow and outflow data based on the urban taxi or bike trajectories. The following datasets are considered: NYCTaxi150103 [59], NYCTaxi160102 [34], NYCTaxi140103*, TaxiBJ2014 [72], TaxiBJ2015 [72], NYCBike160708 [59], NYCBike140409 [72], BikeDC*, BikeCHI*, and NYCBike200709*.

5.2 Models

We conducted experiments on the following 18 models that can be divided into six categories as follows:

(1) General Time Series Prediction Models

- Seq2Seq [46]: uses the encode-decoder framework based on the gated recurrent unit.
- AutoEncoder [40]: uses an encoder to learn the embedding and then a decoder to predict the future.
- FNN [32]: Feed forward neural network with two hidden layers and L2 regularization.

(2) Sequential Structure Models (Spatial-CNNs plus others)

- STResNet [72] models the spatial-temporal correlations by residual unit.
- ACFM [38]: infers the evolution of the crowd flow with a ConvLSTM and attention mechanism
- DMVSTNet [60] combines CNN and LSTM to capture the spatial, temporal, and semantic views.

(3) Sequential Structure Models (Spatial-GCNs plus others)

- STGCN [66] combines GCNs and gated temporal convolution.
- GWNET [56] combines adaptive adjacency matrix into GCNs and 1D dilated casual convolutions.
- MTGNN [55] combines adaptive GCNs with mix-hop propagation layers and dilated inception layers.
- TGCN [75] combines GCNs and the gated recurrent unit.

(4) Sequential Structure Models (Spatial-Attentions plus others)

- ASTGCN [18] pluses the STGCN with spatial-temporal attention mechanism.
- GMAN [76] consists of multiple spatial-temporal attention blocks in the encoder-decoder framework.
- STTN [57] combines the spatial and temporal transformer and graph convolutional network.

(5) Coupled Structure Models (GCNs + RNNs)

- DCRNN [32]: couples the diffusion GCN and the encoder-decoder framework.
- AGCRN [2]: couples the adaptive GCN and the gated recurrent unit.

(6) Spatial-Temporal Synchronized Learning Models

- STG2Seq [1] utilizes a hierarchical graph convolutional to capture spatial and temporal correlations simultaneously.
- STSGCN [45] utilizes spatial-temporal synchronous modeling mechanism to model localized correlations.
- D2STGNN [44] utilizes the diffusion and inherent modules to model the diffusion process and the inherent signal.

5.3 Experimental Settings

5.3.1 Environment Settings. All experiments are conducted using NVIDIA 3090 GPUs and 256 GB memory on Ubuntu 20.04. We complete the implementation of the models with the help of the LibCity [51] framework, using Python 3.9.7 and PyTorch 1.10.1 [42].

5.3.2 Dataset Processing. The datasets are split into training, validation, and test sets with a ratio of 7:1:2. For graph relation Data, we perform multi-step prediction using 12 past steps to predict 12 future steps. For grid relation Data, we perform single-step prediction using six past steps to predict the traffic inflow and outflow of the next single step.

5.3.3 Model and Training Settings. The Adam optimizer is used with a batch size of 64 (adjusted as necessary when OOM occurred for some large models), a training epoch of 100, and an early stopping mechanism when the valid set loss lasts 30 epochs without dropping. Gradient clipping with a gradient clipping value of 5 is employed. The model parameters are set according to the settings in the original paper. Additionally, the time of day is introduced

Table 4: Model Performance Leaderboard

1	2	3	4	5	6
D2STGNN	MTGNN	GWNET	AGCRN	GMAN	DCRNN
7	8	9	10	11	12
STGCN	STTN	STSGCN	STG2Seq	ASTGCN	TGCN
13	14	15	16	17	18
DMVSTNet	ACFM	STResNet	Seq2Seq	FNN	AutoEncoder

as auxiliary data to enhance prediction accuracy, following [56]. To ensure a fair comparison, only the recent components of the ASTGCN [18] and ST-ResNet [72] models are utilized.

5.3.4 Evaluation Metrics. Three widely-used metrics are employed to evaluate the models: (1) Mean Absolute Error (MAE), (2) Mean Absolute Percentage Error (MAPE), and (3) Root Mean Squared Error (RMSE). Missing values are excluded from training and testing, following [32]. For grid relation datasets, samples with flow values below five are filtered, consistent with [60]. Due to spatial constraints, for graph relation data, the reported results are the average of multi-step predictions, while for grid relation data, the reported results are the average of inflows and outflows. We repeat all experiments five times and report the average results.

5.4 Performance Comparison

Table 4 represents the model performance leaderboard for all models on all datasets. Tables 5 and Table 6 present the experiment results for graph relation data and grid relation data, respectively. From these results, we draw the following observations:

(1) General time series prediction models, including Seq2Seq, AutoEncoder, and FNN, perform poorly on urban spatial-temporal data due to ignoring spatial correlation. This suggests that incorporating spatial correlation is crucial to improve prediction accuracy.

(2) The spatial-CNN-based sequential structure models, such as STResNet, ACFM, and DMVSTNet, are only suitable for grid relation data as CNNs can not handle the graph relation data. Although these models are designed for grid data, they perform worse than the spatial-GCN-based models. One possible reason is that the original versions of such models require the input of information from more distant historical data, such as data from the same time period a day ago or a week ago. However, in our experiments, we have removed such information to ensure fair comparisons among the models. Another reason could be that graph neural networks have the ability to capture spatial correlations from grid data if an appropriate graph structure is constructed. This advantage could contribute to the better performance of spatial-GCN-based models.

(3) After analyzing the results from all the tables, we conclude that D2STGNN is the top-performing model. D2STGNN stands out due to its utilization of spatial-temporal synchronized learning and its systematic design of diffusion and inherent modules, tailored to the unique characteristics of spatial-temporal diffusion signals and inherent signals. In particular, each spatial-temporal signal consists of both a diffusion signal, which captures the information diffused from other sensors, and an inherent signal, which captures the information that is independent of other sensors. D2STGNN incorporates a residual decomposition mechanism that effectively

separates the spatial-temporal signals. This allows more precise modeling of the different parts of spatial-temporal data to improve prediction accuracy.

(4) Moving on, MTGNN and GWNET are ranked 2nd and 3rd, respectively. Both models, MTGNN and GWNET, fall under the category of sequential structure models that combine Graph Convolutional Networks (GCNs) with multi-layer Dilated Casual Convolution (also known as WaveNet). They also incorporate an adaptive graph structure learning module within the graph convolution component to address the limitations of fixed graph structures used in DCRNN and STGCN. Additionally, these models employ direct prediction instead of a recurrent approach, which helps mitigate the issue of cumulative errors. MTGNN and GWNET consistently demonstrate strong performance across different datasets. This highlights the potential of combining GCNs with WaveNetS as a promising research direction for future advancements in macro spatial-temporal prediction. Several recent works have also adopted a similar structure, further reinforcing its effectiveness [22, 61].

(5) After this, the 4th ranked model is AGCRN. Both AGCRN and DCRNN employ the coupled structure, which combines Graph Convolutional Networks (GCNs) with Recurrent Neural Networks (RNNs). AGCRN outperforms DCRNN by introducing a learnable graph structure and adopting direct prediction instead of recurrent prediction. On the other hand, models that utilize sequential structures combining GCNs and RNNs, such as TGCN, achieve slightly lower performance. This suggests that the coupled structure is more suitable for integrating GCNs and RNNs compared to sequential structures. It is worth noting that the top 4 models in the overall ranking all use direct prediction. The direct prediction approach involves using two fully-connected layers on the learned hidden states to make multi-step predictions directly without relying on the results of previous steps for the recurrent prediction. This approach helps alleviate the problem of cumulative errors and is more suitable for short-term prediction scenarios such as the urban spatial-temporal prediction.

(6) As a sequential structure model that combines spatial attention with other components, GMAN ranks 5th overall. GMAN utilizes temporal and spatial attention mechanisms to learn spatial-temporal correlations in the data, resulting in a good performance. However, the model has high complexity and consumes a large amount of memory. The other two attention-based models, namely STTN and ASTGCN, perform worse than GMAN, which could be attributed to differences in how attention is computed. GMAN employs a structure based entirely on attention mechanisms and introduces multi-head attention and group attention, while STTN and ASTGCN have a simpler implementation of attention. The main limitation of attention-based models is their high time complexity. Future studies can focus on reducing the complexity of the model and achieving a balance between performance and efficiency.

(7) Lastly, it is worth noting that other models employing spatial-temporal synchronized learning, such as STG2Seq and STSGCN, exhibit slightly lower performance. This can be attributed to their focus on short-range spatial-temporal correlations while overlooking long-range correlations. On the other hand, models like MTGNN and GWNET, which utilize the multi-layer WaveNet architecture, aim to capture long-range temporal correlations. Additionally, recent studies have also highlighted the significance of long-range

Table 5: Performance Comparison on Graph Relation Data

Dataset	METR-LA			PEMS-BAY			PEMSD7(M)			PEMSD4-Speed			PEMSD8-Speed			
Metric	MAE	MAPE	RMSE	MAE	MAPE	RMSE	MAE	MAPE	RMSE	MAE	MAPE	RMSE	MAE	MAPE	RMSE	RANK
Seq2Seq	4.65	11.39	7.79	2.57	6.07	5.32	8.92	21.90	11.47	2.26	5.08	4.88	1.91	4.62	4.63	13
AutoEncoder	4.11	12.01	7.76	2.52	6.13	5.20	8.97	20.18	11.65	2.33	5.45	5.14	2.17	5.22	5.22	15
FNN	4.35	12.73	8.37	2.05	6.16	4.69	8.82	20.16	11.46	1.98	5.36	5.17	1.89	4.72	5.08	14
STGCN	3.29	8.80	6.59	1.71	3.83	3.91	8.44	18.71	9.99	1.71	3.64	3.72	1.42	3.32	3.42	8
GWNET	3.07	8.32	6.16	1.58	3.56	3.55	8.07	18.56	10.39	1.57	3.32	3.60	1.29	2.88	3.23	2
MTGNN	3.02	8.25	6.09	1.59	3.59	3.58	8.02	18.33	9.86	1.60	3.42	3.69	1.29	2.89	3.21	3
TGCN	3.52	9.93	6.87	1.82	4.24	3.85	8.74	18.91	11.37	1.90	3.80	3.75	1.73	3.79	3.50	12
ASTGCN	3.47	9.82	6.73	1.90	4.28	4.25	8.50	19.51	11.33	1.79	3.82	3.74	1.49	3.32	3.49	11
GMAN	3.16	8.65	6.43	1.57	3.65	3.64	7.67	18.04	9.76	1.68	3.65	3.63	1.35	3.13	3.21	5
STTN	3.26	9.07	6.54	1.68	3.81	3.85	8.70	18.99	10.87	1.64	3.45	3.68	1.42	3.47	3.68	7
DCRNN	3.16	8.66	6.44	1.67	3.80	3.83	8.52	19.58	10.46	1.65	3.46	3.76	1.40	3.10	3.43	6
AGCRN	3.17	8.79	6.35	1.62	3.68	3.63	7.76	18.19	10.39	1.62	3.41	3.64	1.34	3.01	3.27	4
STG2Seq	3.41	9.33	6.64	1.76	3.84	3.94	8.43	19.85	10.53	1.85	3.60	3.79	1.59	3.58	3.74	10
STSGCN	3.34	9.26	6.65	1.75	3.81	3.90	8.08	19.55	10.98	1.84	3.55	3.73	1.53	3.51	3.73	9
D2STGNN	2.91	7.93	5.84	1.56	3.59	3.46	2.49	6.26	5.03	1.55	3.28	3.50	1.28	3.07	3.32	1

Dataset	PEMSD4-Flow			PEMSD8-Flow			PEMSD4-Occupy			PEMSD8-Occupy			PEMSD3			
Metric	MAE	MAPE	RMSE	MAE	MAPE	RMSE	MAE	MAPE	RMSE	MAE	MAPE	RMSE	MAE	MAPE	RMSE	RANK
Seq2Seq	22.84	16.30	36.72	20.35	12.79	33.15	0.93	20.70	2.40	0.89	14.46	2.39	20.07	19.55	34.22	13
AutoEncoder	24.42	17.83	38.38	21.32	13.73	35.11	0.98	21.25	2.49	0.99	15.91	2.57	23.12	23.36	38.36	15
FNN	24.17	17.73	39.48	20.74	13.21	32.03	0.94	21.42	2.29	0.83	15.41	2.18	20.50	19.59	33.20	14
STGCN	20.39	13.95	32.41	15.63	10.50	24.63	0.77	16.52	2.08	0.71	11.54	1.89	15.81	15.31	27.10	7
GWNET	18.64	13.36	30.03	14.51	9.39	23.36	0.73	16.32	1.95	0.65	10.68	1.85	14.50	13.97	24.98	1
MTGNN	18.68	13.99	30.05	14.88	9.93	23.81	0.73	16.15	1.93	0.66	10.87	1.85	14.78	14.16	25.61	3
TGCN	20.91	14.80	33.38	16.26	11.86	25.65	0.84	17.71	2.15	0.77	12.14	1.94	16.98	18.62	28.26	12
ASTGCN	20.37	14.24	32.73	16.36	11.89	24.95	0.83	17.67	2.17	0.75	11.95	1.92	16.80	16.35	27.71	10
GMAN	19.44	14.52	30.79	15.67	10.99	24.20	0.75	16.76	2.01	0.66	11.59	1.85	15.60	16.33	27.30	5
STTN	19.89	14.67	31.14	16.10	11.28	24.70	0.79	17.16	2.11	0.70	11.58	1.94	16.07	17.41	27.93	8
DCRNN	19.97	13.87	31.53	15.45	9.86	24.11	0.75	16.85	2.03	0.69	11.38	1.87	15.66	16.39	27.92	6
AGCRN	18.74	12.81	30.60	14.84	9.93	24.06	0.74	16.59	1.96	0.68	11.52	1.85	15.21	15.03	27.02	4
STG2Seq	20.13	14.90	31.36	16.27	11.32	24.93	0.82	17.64	2.18	0.73	11.97	1.97	16.44	16.41	28.13	11
STSGCN	20.15	14.60	31.27	16.16	11.29	24.82	0.81	17.40	2.17	0.73	11.91	1.95	16.36	16.37	28.11	9
D2STGNN	18.47	13.04	30.19	14.67	9.67	23.50	0.73	16.24	1.93	0.67	11.17	1.81	14.66	14.70	25.81	2

spatial dependencies in spatial-temporal prediction [28, 29]. These findings further emphasize the importance of considering both short- and long-range correlations in spatial-temporal modeling and prediction tasks.

5.5 Model Efficiency Study

Table 7 displays the training and inference time for each epoch, separately for graph relation data and grid relation data. Due to limited space, only the results of 12 datasets are provided here. However, it is important to note that other datasets typically exhibit similar efficiency performance to those shown in Table 7, such as PEMS4-Flow, PEMS4-Occupy, and PEMS4-Speed. Throughout the experiment, we use a consistent batch size of 16 to prevent GPU memory consumption from surpassing the capacity of a single card. Based on these results, we can make the following observations:

(1) General time series prediction models that do not consider spatial dependencies between spatial entities generally exhibit noticeably faster training and inference times compared to others.

(2) Among the three spatial-CNNs-based sequential structure models, STResNet stands out for its relatively high computational efficiency. This is primarily attributed to its utilization of convolution-based residual networks, which are computationally efficient compared to models incorporating RNNs and attention mechanisms like ACFM and DMVSTNet.

(3) In terms of other sequential structure models, spatial GCN-based models such as STGCN, GWNET, MTGNN and TGCN demonstrate superior computational efficiency in comparison to spatial-attention-based models such as GMAN and STTN, especially when dealing with large graphs such as TaxiBJ2014 (1024 nodes). This is primarily because spatial-attention-based models require calculating attention between each spatial entity and all other spatial entities, leading to higher computational costs. In contrast, spatial-GCN-based models typically focus solely on the spatial dependencies of neighboring spatial entities within a specific distance or number of hops for each spatial entity. As a result, they incur significantly lower computational costs. These spatial-attention-based models prioritize performance over computational efficiency. While

Table 6: Performance Comparison on Grid Relation Data

Dataset	NYCTaxi150103			NYCTaxi160102			NYCTaxi140103			TaxiBJ2014			TaxiBJ2015			
Metric	MAE	MAPE	RMSE	MAE	MAPE	RMSE	MAE	MAPE	RMSE	MAE	MAPE	RMSE	MAE	MAPE	RMSE	RANK
Seq2Seq AutoEncoder FNN	12.95	20.21	21.23	12.89	20.35	21.23	8.92	21.90	11.47	16.94	18.93	21.93	18.29	21.16	27.88	18
	12.56	20.86	21.90	12.83	20.11	22.37	8.97	20.18	11.65	15.00	17.31	21.05	18.53	22.57	22.84	17
	14.12	22.32	21.68	13.65	22.22	19.84	8.82	20.16	11.46	14.43	17.52	21.74	15.99	18.69	21.62	16
STResNet ACFM DMVSTNet	12.12	20.18	20.71	11.96	18.81	16.59	9.09	19.96	11.84	11.82	15.64	18.83	12.85	16.87	18.93	15
	12.24	20.06	20.53	11.40	18.78	16.31	8.77	19.70	11.63	11.74	15.83	18.71	12.83	16.33	18.90	14
	11.99	19.97	20.47	11.53	18.61	16.23	8.75	19.66	11.40	11.71	15.64	18.67	12.67	15.24	18.75	13
STGCN GWNEN MTGNN TGCN	10.84	18.48	18.64	10.68	18.58	14.95	8.44	18.71	9.99	11.47	14.46	18.63	11.62	14.58	17.34	7
	10.24	17.37	16.71	10.48	17.98	15.28	8.07	18.56	10.39	11.43	13.98	18.34	11.22	14.71	18.38	5
	10.42	17.19	15.80	10.00	16.80	14.50	8.02	18.33	9.86	11.48	14.05	17.38	11.03	14.37	17.05	1
	11.97	18.93	20.27	10.11	18.16	14.86	8.74	18.91	11.37	11.62	15.59	18.18	11.87	15.11	18.72	12
ASTGCN GMAN STTN	11.97	19.99	20.32	10.48	18.19	14.83	8.50	19.51	11.33	11.44	14.35	18.33	12.27	15.27	17.63	11
	9.83	17.62	15.53	9.61	17.60	14.12	7.67	18.04	9.76	11.48	14.26	18.05	11.23	15.17	17.58	4
	10.55	20.05	17.20	9.86	18.73	14.50	8.70	18.99	10.87	11.20	15.15	18.62	11.36	15.02	18.04	8
DCRNN AGCRN	10.00	17.81	14.86	9.82	17.53	14.00	8.52	19.58	10.46	11.68	14.70	17.44	11.36	15.11	17.56	6
	10.02	17.52	17.92	9.79	17.30	14.39	7.76	18.19	10.39	11.40	14.14	18.25	11.12	14.48	18.06	3
STG2Seq STSGCN D2STGNN	11.21	18.82	18.27	11.27	17.63	15.41	8.43	19.85	10.53	11.63	14.36	18.52	11.33	15.21	18.10	10
	10.93	18.95	16.94	10.28	17.74	15.24	8.08	19.55	10.98	11.69	14.38	18.53	11.56	15.11	18.45	9
	10.24	17.53	16.53	10.05	17.33	14.41	7.67	17.15	9.83	11.44	14.17	17.62	11.15	14.52	17.53	2

Dataset	NYCBike160708			NYCBike140409			NYCBike200709			BikeDC			BikeCHI			
Metric	MAE	MAPE	RMSE	MAE	MAPE	RMSE	MAE	MAPE	RMSE	MAE	MAPE	RMSE	MAE	MAPE	RMSE	RANK
Seq2Seq AutoEncoder FNN	5.61	26.14	7.35	5.61	25.83	7.81	8.57	25.52	14.34	10.88	34.97	15.09	5.80	27.92	8.53	16
	5.81	26.79	7.55	5.63	25.72	7.89	8.59	25.54	14.58	10.94	32.57	14.83	5.88	28.72	8.68	17
	5.80	27.12	7.90	6.15	25.59	7.77	8.62	25.43	14.72	10.87	32.77	14.99	6.12	29.38	8.78	18
STResNet ACFM DMVSTNet	5.53	25.85	7.05	5.86	26.63	7.97	8.86	25.40	14.18	10.77	30.38	14.89	5.62	27.19	7.96	15
	5.64	25.89	6.87	5.68	26.30	7.85	8.75	25.38	14.27	10.73	30.25	14.83	5.54	26.66	7.90	14
	5.32	25.80	6.76	5.63	26.29	7.75	8.70	25.32	14.08	10.67	30.15	14.70	5.53	26.41	7.71	13
STGCN GWNEN MTGNN TGCN	4.64	23.21	6.53	5.31	24.96	6.91	7.52	22.30	11.31	10.10	27.13	13.66	4.67	24.84	6.42	7
	4.55	23.22	6.48	5.19	24.19	6.85	7.47	22.38	11.11	10.14	26.30	12.88	4.72	24.61	6.24	5
	4.49	22.58	5.87	4.94	23.57	6.41	7.10	21.97	10.36	9.96	26.89	12.68	4.50	24.60	5.69	1
	4.82	25.81	6.51	5.46	24.43	7.07	8.55	25.34	13.74	10.06	29.68	14.63	5.51	26.40	6.77	12
ASTGCN GMAN STTN	5.22	24.53	6.68	5.57	24.13	7.44	8.27	25.21	13.82	10.16	29.04	14.34	5.42	26.41	5.87	11
	4.53	22.90	5.95	5.03	24.44	6.85	7.43	22.24	11.40	9.87	26.11	12.11	4.75	24.60	6.25	3
	4.65	24.22	6.37	5.14	25.24	6.80	7.50	23.49	11.72	9.97	27.79	12.22	4.81	25.75	6.60	8
DCRNN AGCRN	4.50	23.13	6.38	5.12	24.47	6.93	7.44	22.43	11.42	9.95	27.11	13.26	4.73	25.62	6.21	6
	4.52	23.02	5.97	5.13	24.43	6.65	7.54	22.38	11.45	9.96	27.57	12.62	4.78	25.61	6.11	4
STG2Seq STSGCN D2STGNN	5.08	24.26	6.74	5.41	24.46	7.09	8.04	25.05	11.93	10.11	28.09	13.77	4.80	25.86	6.58	10
	4.63	23.66	6.64	5.40	24.67	7.18	7.62	23.16	11.81	9.97	27.61	12.99	4.81	26.21	6.44	9
	4.65	22.75	6.12	4.98	23.50	6.44	7.30	22.86	10.64	9.30	25.16	11.69	4.68	25.35	5.96	2

they may have lower computational efficiency, they aim to deliver superior model performance.

(4) The sequential structure models such as STGCN, GWNEN, and MTGNN tend to have shorter training and inference times compared to coupled structure models such as DCRNN and AGCRN in general. This is mainly due to the utilization of Temporal Convolutional Networks (TCNs) in sequential models, which generally offer faster computation compared to the Recurrent Neural Networks (RNNs) used in coupled structure models.

(5) When conducting multi-step predictions, recurrent prediction models such as DCRNN and GMAN exhibit significantly longer training and inference times compared to direct prediction models

like GWNEN, MTGNN, TGCN, and ASTGCN. The recurrent prediction models typically follow an encoder-decoder architecture and generate predictions based on previous predictions, making them unsuitable for parallel computation and resulting in increased computational complexity. However, the direct prediction models can predict the results of multiple steps at once, leading to faster training and inference times.

(6) The relatively low efficiency of spatial-temporal synchronous modeling models, such as STG2Seq, STSGCN, and D2STGNN, can be attributed to the inclusion of more complex spatial-temporal joint learning modules. Only some of the larger models are less efficient than them, such as DCRNN and GMAN, but both are mainly limited by the paradigm of recurrent prediction. Although

Table 7: Comparison of Training and Inference Time Per Epoch (Unit: seconds)

Dataset	METR-LA		PEMS-BAY		PEMSD7(M)		PEMSD3		PEMSD4-Flow		PEMSD8-Flow		RANK	
Model	Train	Infer	Train	Infer	Train	Infer	Train	Infer	Train	Infer	Train	Infer	Train	Infer
Seq2Seq AutoEncoder FNN	20.94	0.86	32.85	1.35	7.14	0.33	13.32	0.69	8.41	0.43	10.16	0.48	3	3
	6.84	0.38	10.51	0.69	2.65	0.15	5.40	0.37	3.68	0.23	3.29	0.15	2	2
	5.72	0.35	9.18	0.65	2.27	0.14	4.74	0.35	3.32	0.21	3.01	0.17	1	1
STGCN	25.85	9.99	41.66	14.97	10.68	3.50	18.85	7.55	12.88	4.94	12.91	4.94	4	12
GWNET	91.45	2.86	153.21	4.95	36.37	1.17	61.86	2.43	44.86	1.64	42.97	1.42	8	5
MTGNN	75.64	2.73	121.95	4.29	27.14	0.99	60.15	2.29	38.22	1.45	37.67	1.28	5	4
TGCN	64.50	5.75	102.07	9.03	27.16	1.93	62.60	4.02	39.45	2.92	38.49	2.45	6	7
ASTGCN	90.67	4.91	145.59	8.71	34.28	1.88	74.26	4.68	46.44	2.80	42.71	2.26	7	6
GMAN	738.24	14.57	1950.34	40.04	298.04	5.98	1116.30	22.57	579.96	11.88	326.05	6.34	15	14
STTN	166.38	7.51	274.66	14.62	61.09	2.83	145.01	7.83	86.71	4.55	84.52	3.66	11	9
DCRNN	605.88	37.18	967.10	60.29	340.60	23.08	490.85	32.16	294.00	18.76	319.62	19.61	14	15
AGCRN	156.36	8.24	251.72	15.41	59.22	3.12	128.18	7.16	82.38	4.92	82.39	4.08	9	10
STG2Seq	164.39	9.24	261.81	15.52	59.87	3.27	135.30	7.92	85.77	4.78	84.23	4.31	10	11
STSGCN	181.62	5.94	269.59	8.61	66.32	2.08	142.72	4.78	89.58	2.84	94.06	3.48	12	8
D2STGNN	259.78	10.97	430.64	19.36	99.41	4.60	222.67	10.32	139.02	6.68	135.44	5.40	13	13

Dataset	NYCTaxi140103		NYCTaxi160102		NYCBike140409		NYCBike160708		TaxiBJ2014		BikeCHI		RANK	
Model	Train	Infer	Train	Infer	Train	Infer	Train	Infer	Train	Infer	Train	Infer	Train	Infer
Seq2Seq AutoEncoder FNN	0.40	0.02	0.73	0.04	0.97	0.04	0.62	0.03	1.25	0.09	0.48	0.03	3	3
	0.30	0.02	0.45	0.02	0.65	0.03	0.51	0.02	1.03	0.07	0.34	0.02	2	2
	0.25	0.02	0.36	0.02	0.51	0.03	0.37	0.02	0.86	0.07	0.28	0.02	1	1
STResNet	2.45	0.11	3.63	0.16	4.49	0.25	3.68	0.17	5.97	0.29	2.76	0.13	5	7
ACFM	14.23	0.52	15.69	0.68	23.17	1.05	18.67	0.65	25.40	1.13	12.02	0.53	16	15
DMVSTNet	36.48	2.11	50.25	2.81	38.99	2.20	50.33	2.80	611.21	35.47	59.99	3.42	18	18
STGCN	1.41	0.07	2.16	0.08	3.04	0.14	2.01	0.08	6.11	0.19	1.72	0.08	4	4
GWNET	2.55	0.09	3.20	0.12	4.57	0.19	3.42	0.11	13.00	0.31	2.67	0.09	7	5
MTGNN	2.71	0.10	3.19	0.13	5.38	0.18	3.61	0.13	8.83	0.57	2.55	0.09	8	6
TGCN	2.63	0.12	3.57	0.16	4.63	0.21	3.47	0.15	6.10	0.69	2.71	0.14	6	9
ASTGCN	2.46	0.14	3.45	0.18	5.05	0.27	3.57	0.17	9.86	0.68	2.89	0.14	9	10
GMAN	21.00	0.65	28.12	0.84	36.72	1.28	28.67	0.88	172.37	6.06	26.18	0.69	17	17
STTN	6.77	0.28	9.57	0.37	14.53	0.57	9.43	0.38	47.61	2.56	7.49	0.33	14	14
DCRNN	10.26	0.67	13.70	0.81	21.78	1.31	14.78	0.88	26.29	1.85	10.42	0.65	15	16
AGCRN	2.79	0.13	3.13	0.18	5.63	0.28	3.72	0.18	11.21	0.37	2.45	0.15	10	11
STG2Seq	3.23	0.14	3.88	0.16	5.92	0.23	3.82	0.15	10.92	0.69	3.07	0.13	11	8
STSGCN	3.55	0.14	4.48	0.18	7.76	0.29	5.00	0.19	11.71	0.61	3.87	0.15	12	13
D2STGNN	3.49	0.14	5.18	0.17	7.83	0.26	5.32	0.18	22.54	1.16	3.97	0.15	13	12

D2STGNN is the top model in terms of performance, its efficiency is far from that of MTGNN and GWNET, which rank 2nd and 3rd. When selecting a model for a particular application, it is critical to consider the requirements of the scenario, taking into account both efficiency and performance to make the appropriate decision.

5.6 Analysis of Prediction Results and Performance Discrepancies

We select the best-performing models from each category according to Table 4 and visualize their prediction results on the METR-LA and PEMS8-Speed datasets for different times and days

in Figure 3(1) and Figure 3(2) respectively. For each dataset, we plot four subplots: (a) and (b) show the trend of average traffic speed at different times of the day and different days of the week, respectively; (c) and (d) show the mean absolute percentage error (MAPE) between the model’s prediction and the ground truth at different times on weekdays and weekends, respectively.

From subfigures (a) and (b), we observe peak periods and periodicity in the real data. The peak periods are typically concentrated around 8:00 and 17:00, while the data exhibits periodic patterns on weekdays and weekends, respectively. Furthermore, the traffic speed distribution on weekends appears more concentrated, with

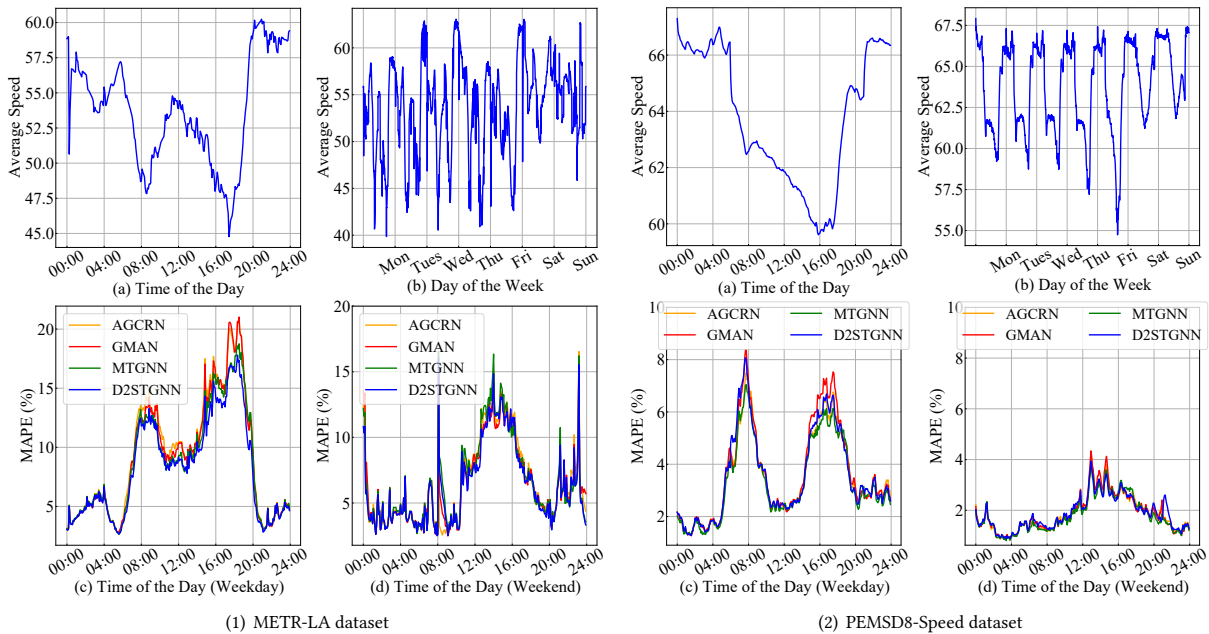


Figure 3: Data distribution and model performance of the METR-LA and PEMS8-Speed at different time periods.

a smaller variance than on weekdays. Correspondingly, according to subfigures (c) and (d), there is a significant difference in the performance of the models on weekdays and weekends. The models perform better on weekends, which can be attributed to the more concentrated data distribution during those periods. On weekdays, however, the selected models achieve relatively similar performance during non-peak periods, while there is a noticeable performance gap during peak periods. The main source of the performance gap among these four models is their performance during peak periods.

As shown in subfigures (a) and (b), traffic conditions during peak periods tend to exhibit more complex and rapid changes, with a higher likelihood of extreme situations such as traffic congestion or accidents. Therefore, predicting traffic during peak periods is more challenging than during other periods. However, in practical applications, accurate traffic predictions during peak periods are precisely what people are more concerned about. These figures also indicate that improving the overall performance of the models relies on enhancing their prediction accuracy during peak periods. These observations provide researchers with a direction for the future design and development of better traffic models, focusing on capturing the fluctuations in traffic conditions during peak periods.

6 CONCLUSION

6.1 Limitations and Future Work

It is important to acknowledge the limitations of this study. This paper primarily focuses on traffic prediction in the transportation field within the realm of urban spatial-temporal prediction while giving less attention to other related fields such as air quality prediction, climate prediction, and crime frequency prediction. This choice is driven by the fact that traffic prediction is one of the most critical and rapidly evolving domains within urban spatial-temporal prediction. However, it is essential to highlight that the proposed "atomic files" format is not exclusively limited to traffic data. It can

be applied to various other types of urban spatial-temporal data, including temperature, wind speed, crime incidents, and more.

Exploring other domains of spatial-temporal prediction tasks, such as meteorology, is a potential avenue for future work. Expanding the scope of research to encompass a broader range of prediction tasks will contribute to a more comprehensive understanding of urban spatial-temporal dynamics and facilitate technique advancements in various fields. Future work will involve exploring additional areas of spatial-temporal prediction, expanding the utility of this work, and further enhancing our understanding of spatial-temporal dynamics in different contexts.

6.2 Conclusion

In conclusion, this work addresses the challenges faced in the field of urban spatial-temporal prediction and makes significant contributions to data management and prediction techniques. By introducing the unified storage format "atomic files," we simplify the access and utilization of diverse urban spatial-temporal datasets, enhancing data management efficiency. The comprehensive overview of technological advances in prediction models provides researchers with valuable insights and guidance for developing robust models. Additionally, the extensive experiments conducted using diverse models and datasets establish a performance benchmark and identify promising research directions.

Looking ahead, the findings and methodologies presented in this work pave the way for future research in urban spatial-temporal prediction. Researchers and practitioners can leverage the unified storage format and technological roadmap and model performance benchmark to explore new avenues, develop innovative models, and contribute to the advancement of the field. Ultimately, these efforts will lead to more effective management of urban spatial-temporal data, enhanced prediction capabilities, and improved urban planning and development.

REFERENCES

- [1] Lei Bai, Lina Yao, Salil S. Kanhere, Xianzhi Wang, and Quan Z. Sheng. 2019. STG2Seq: Spatial-Temporal Graph to Sequence Model for Multi-step Passenger Demand Forecasting. In *IJCAI*. ijcai.org, 1981–1987.
- [2] Lei Bai, Lina Yao, Can Li, Xianzhi Wang, and Can Wang. 2020. Adaptive Graph Convolutional Recurrent Network for Traffic Forecasting. *NIPS* 33 (2020).
- [3] Weiqi Chen, Ling Chen, Yu Xie, Wei Cao, Yusong Gao, and Xiaojie Feng. 2020. Multi-Range Attentive Bicomponent Graph Convolutional Network for Traffic Forecasting. In *AAAI*. AAAI Press, 3529–3536.
- [4] Jeongwhan Choi, Hwangyong Choi, Jeehyun Hwang, and Noseong Park. 2022. Graph Neural Controlled Differential Equations for Traffic Forecasting. In *AAAI*. AAAI Press, 6367–6374.
- [5] Junyoung Chung, Çağlar Gülçehre, KyungHyun Cho, and Yoshua Bengio. 2014. Empirical Evaluation of Gated Recurrent Neural Networks on Sequence Modeling. *CoRR* abs/1412.3555 (2014).
- [6] Yue Cui, Kai Zheng, Dingshan Cui, Jiandong Xie, Liwei Deng, Feiteng Huang, and Xiaofang Zhou. 2021. METRO: A Generic Graph Neural Network Framework for Multivariate Time Series Forecasting. *Proc. VLDB Endow.* 15, 2 (2021), 224–236.
- [7] Zhiyong Cui, Kristian Henriksson, Ruimin Ke, and Yinhai Wang. 2019. Traffic graph convolutional recurrent neural network: A deep learning framework for network-scale traffic learning and forecasting. *IEEE Transactions on Intelligent Transportation Systems* 21, 11 (2019), 4883–4894.
- [8] Zhiyong Cui, Ruimin Ke, and Yinhai Wang. 2018. Deep Bidirectional and Unidirectional LSTM Recurrent Neural Network for Network-wide Traffic Speed Prediction. *CoRR* abs/1801.02143 (2018).
- [9] Rodrigo de Medrano and José Luis Aznarte. 2020. A Spatio-Temporal Spot-Forecasting Framework for Urban Traffic Prediction. *CoRR* abs/2003.13977 (2020).
- [10] Michaël Defferrard, Xavier Bresson, and Pierre Vandergheynst. 2016. Convolutional Neural Networks on Graphs with Fast Localized Spectral Filtering. In *NIPS*. 3837–3845.
- [11] Zulong Diao, Xin Wang, Dafang Zhang, Yingru Liu, Kun Xie, and Shaoyao He. 2019. Dynamic Spatial-Temporal Graph Convolutional Neural Networks for Traffic Forecasting. In *AAAI*. AAAI Press, 890–897.
- [12] Harris Drucker, Christopher J. C. Burges, Linda Kaufman, Alexander J. Smola, and Vladimir Vapnik. 1996. Support Vector Regression Machines. In *NIPS*. MIT Press, 155–161.
- [13] Zheng Fang, Qingqing Long, Guojie Song, and Kunqing Xie. 2021. Spatial-Temporal Graph ODE Networks for Traffic Flow Forecasting. In *KDD*. ACM, 364–373.
- [14] Ziquan Fang, Lu Pan, Lu Chen, Yuntao Du, and Yunjun Gao. 2021. MDTP: A Multi-source Deep Traffic Prediction Framework over Spatio-Temporal Trajectory Data. *Proc. VLDB Endow.* 14, 8 (2021), 1289–1297.
- [15] Ke Gu, Jieyu Hu, and Weijia Jia. 2023. Adaptive Area-Based Traffic Congestion Control and Management Scheme Based on Fog Computing. *IEEE Trans. Intell. Transp. Syst.* 24, 1 (2023), 1359–1373.
- [16] Kan Guo, Yongli Hu, Zhen Sean Qian, Yanfeng Sun, Junbin Gao, and Baocai Yin. 2022. Dynamic Graph Convolution Network for Traffic Forecasting Based on Latent Network of Laplace Matrix Estimation. *IEEE Trans. Intell. Transp. Syst.* 23, 2 (2022), 1009–1018.
- [17] Kan Guo, Yongli Hu, Yanfeng Sun, Sean Qian, Junbin Gao, and Baocai Yin. 2021. Hierarchical graph convolution network for traffic forecasting. In *Proceedings of the AAAI conference on artificial intelligence*, Vol. 35. 151–159.
- [18] Shengnan Guo, Youfang Lin, Ning Feng, Chao Song, and Huaiyu Wan. 2019. Attention based spatial-temporal graph convolutional networks for traffic flow forecasting. In *Proceedings of the AAAI Conference on Artificial Intelligence*, Vol. 33. 922–929.
- [19] Shengnan Guo, Youfang Lin, Huaiyu Wan, Xiucheng Li, and Gao Cong. 2022. Learning Dynamics and Heterogeneity of Spatial-Temporal Graph Data for Traffic Forecasting. *IEEE Trans. Knowl. Data Eng.* 34, 11 (2022), 5415–5428.
- [20] Li Guopeng, Victor L Knoop, and Hans van Lint. 2020. Dynamic Graph Filters Networks: A Gray-box Model for Multistep Traffic Forecasting. In *2020 IEEE 23rd International Conference on Intelligent Transportation Systems (ITSC)*. IEEE, 1–6.
- [21] James Douglas Hamilton. 1994. *Time series analysis*. Princeton university press.
- [22] Liangzhe Han, Bowen Du, Leilei Sun, Yanjie Fu, Yisheng Lv, and Hui Xiong. 2021. Dynamic and Multi-faceted Spatio-temporal Deep Learning for Traffic Speed Forecasting. In *KDD*. ACM, 547–555.
- [23] Liangzhe Han, Xiaojian Ma, Leilei Sun, Bowen Du, Yanjie Fu, Weifeng Lv, and Hui Xiong. 2022. Continuous-Time and Multi-Level Graph Representation Learning for Origin-Destination Demand Prediction. In *KDD*. ACM, 516–524.
- [24] Xiao He, Ye Li, Jian Tan, Bin Wu, and Feifei Li. 2023. OneShotSTL: One-Shot Seasonal-Trend Decomposition For Online Time Series Anomaly Detection And Forecasting. *Proc. VLDB Endow.* 16, 6 (2023), 1399–1412.
- [25] Sepp Hochreiter and Jürgen Schmidhuber. 1997. Long Short-Term Memory. *Neural Comput.* 9, 8 (1997), 1735–1780.
- [26] Jiahao Ji, Jingyuan Wang, Zhe Jiang, Jiawei Jiang, and Hu Zhang. 2022. STDEN: Towards Physics-Guided Neural Networks for Traffic Flow Prediction. In *AAAI*. AAAI Press, 4048–4056.
- [27] Jiahao Ji, Jingyuan Wang, Zhe Jiang, Jingtian Ma, and Hu Zhang. 2020. Interpretable Spatiotemporal Deep Learning Model for Traffic Flow Prediction based on Potential Energy Fields. In *ICDM*. IEEE, 1076–1081.
- [28] Jiawei Jiang, Chengkai Han, and Jingyuan Wang. 2023. BUAA_BIGSCity: Spatial-Temporal Graph Neural Network for Wind Power Forecasting in Baidu KDD CUP 2022. *arXiv preprint arXiv:2302.11159* (2023).
- [29] Jiawei Jiang, Chengkai Han, Wayne Xin Zhao, and Jingyuan Wang. 2023. PDFormer: Propagation Delay-aware Dynamic Long-range Transformer for Traffic Flow Prediction. In *AAAI*. AAAI Press.
- [30] Bohan Li, Tianlun Dai, Weitong Chen, Xinyang Song, Yalei Zang, Zhelong Huang, Qinyong Lin, and Ken Cai. 2023. T-PORP: A Trusted Parallel Route Planning Model on Dynamic Road Networks. *IEEE Trans. Intell. Transp. Syst.* 24, 1 (2023), 1238–1250.
- [31] Mengzhang Li and Zhanxing Zhu. 2021. Spatial-Temporal Fusion Graph Neural Networks for Traffic Flow Forecasting. In *AAAI*. AAAI Press, 4189–4196.
- [32] Yaguang Li, Rose Yu, Cyrus Shahabi, and Yan Liu. 2018. Diffusion Convolutional Recurrent Neural Network: Data-Driven Traffic Forecasting. In *International Conference on Learning Representations (ICLR '18)*.
- [33] Binbing Liao, Jingqing Zhang, Chao Wu, Douglas Mellwraith, Tong Chen, Shengwen Yang, Yike Guo, and Fei Wu. 2018. Deep Sequence Learning with Auxiliary Information for Traffic Prediction. In *Proceedings of the 24th ACM SIGKDD International Conference on Knowledge Discovery and Data Mining*. ACM, 537–546.
- [34] Haoxing Lin, Rufan Bai, Weijia Jia, Xinyu Yang, and Yongjian You. 2020. Preserving Dynamic Attention for Long-Term Spatial-Temporal Prediction. In *KDD*. ACM, 36–46.
- [35] Dachuan Liu, Jin Wang, Shuo Shang, and Peng Han. 2022. MSDR: Multi-Step Dependency Relation Networks for Spatial Temporal Forecasting. In *KDD*. ACM, 1042–1050.
- [36] Lingbo Liu, Jingwen Chen, Hefeng Wu, Jiajie Zhen, Guanbin Li, and Liang Lin. 2020. Physical-Virtual Collaboration Modeling for Intra- and Inter-Station Metro Ridership Prediction. *IEEE Transactions on Intelligent Transportation Systems* (2020).
- [37] Lingbo Liu, Zhilin Qiu, Guanbin Li, Qing Wang, Wanli Ouyang, and Liang Lin. 2019. Contextualized spatial-temporal network for taxi origin-destination demand prediction. *IEEE Transactions on Intelligent Transportation Systems* 20, 10 (2019), 3875–3887.
- [38] Lingbo Liu, Ruimao Zhang, Jiefeng Peng, Guanbin Li, Bowen Du, and Liang Lin. 2018. Attentive crowd flow machines. In *Proceedings of the 26th ACM international conference on Multimedia*. 1553–1561.
- [39] Bin Lu, Xiaoying Gan, Haiming Jin, Luoyi Fu, and Haisong Zhang. 2020. Spatiotemporal Adaptive Gated Graph Convolution Network for Urban Traffic Flow Forecasting. In *CIKM*. ACM, 1025–1034.
- [40] Yisheng Lv, Yanjie Duan, Wenwen Kang, Zhengxi Li, and Fei-Yue Wang. 2014. Traffic flow prediction with big data: a deep learning approach. *IEEE Transactions on Intelligent Transportation Systems* 16, 2 (2014), 865–873.
- [41] Boris N. Oreshkin, Arezou Amini, Lucy Coyle, and Mark Coates. 2021. FC-GAGA: Fully Connected Gated Graph Architecture for Spatio-Temporal Traffic Forecasting. In *AAAI*. AAAI Press, 9233–9241.
- [42] Adam Paszke, Sam Gross, Francisco Massa, Adam Lerer, James Bradbury, Gregory Chanan, Trevor Killeen, Zeming Lin, Natalia Gimelshein, Luca Antiga, Alban Desmaison, Andreas Köpf, Edward Z. Yang, Zachary DeVito, Martin Raison, Alykhan Tejani, Sasank Chilamkurthy, Benoit Steiner, Lu Fang, Junjie Bai, and Soumith Chintala. 2019. PyTorch: An Imperative Style, High-Performance Deep Learning Library. In *NeurIPS*. 8024–8035.
- [43] Han Qiu, Qinkai Zheng, Mounira Msahli, Gérard Memmi, Meikang Qiu, and Jialiang Lu. 2021. Topological Graph Convolutional Network-Based Urban Traffic Flow and Density Prediction. *IEEE Trans. Intell. Transp. Syst.* 22, 7 (2021), 4560–4569.
- [44] Zezhi Shao, Zhao Zhang, Wei Wei, Fei Wang, Yongjun Xu, Xin Cao, and Christian S. Jensen. 2022. Decoupled Dynamic Spatial-Temporal Graph Neural Network for Traffic Forecasting. *Proc. VLDB Endow.* 15, 11 (2022), 2733–2746.
- [45] Chao Song, Youfang Lin, Shengnan Guo, and Huaiyu Wan. 2020. Spatial-temporal synchronous graph convolutional networks: A new framework for spatial-temporal network data forecasting. In *Proceedings of the AAAI Conference on Artificial Intelligence*, Vol. 34. 914–921.
- [46] Ilya Sutskever, Oriol Vinyals, and Quoc V. Le. 2014. Sequence to Sequence Learning with Neural Networks. In *NIPS*. 3104–3112.
- [47] David Alexander Tedjopurnomo, Zhiheng Bao, Baihua Zheng, Farhana Murtaza Choudhury, and Alex Kai Qin. 2022. A Survey on Modern Deep Neural Network for Traffic Prediction: Trends, Methods and Challenges. *IEEE Trans. Knowl. Data Eng.* 34, 4 (2022), 1544–1561.
- [48] Aaron van den Oord, Sander Dieleman, Heiga Zen, Karen Simonyan, Oriol Vinyals, Alex Graves, Nal Kalchbrenner, Andrew W. Senior, and Koray Kavukcuoglu. 2016. WaveNet: A Generative Model for Raw Audio. In *SSW*. ISCA, 125.
- [49] Beibei Wang, Youfang Lin, Shengnan Guo, and Huaiyu Wan. 2021. GSNNet: Learning Spatial-Temporal Correlations from Geographical and Semantic Aspects for Traffic Accident Risk Forecasting. In *AAAI*. AAAI Press, 4402–4409.

- [50] Jingyuan Wang, Qian Gu, Junjie Wu, Guannan Liu, and Zhang Xiong. 2016. Traffic Speed Prediction and Congestion Source Exploration: A Deep Learning Method. In *ICDM*. IEEE Computer Society, 499–508.
- [51] Jingyuan Wang, Jiawei Jiang, Wenjun Jiang, Chao Li, and Wayne Xin Zhao. 2021. LibCity: An Open Library for Traffic Prediction. In *SIGSPATIAL/GIS*. ACM, 145–148.
- [52] Senzhang Wang, Jiannong Cao, and Philip S. Yu. 2022. Deep Learning for Spatio-Temporal Data Mining: A Survey. *IEEE Trans. Knowl. Data Eng.* 34, 8 (2022), 3681–3700.
- [53] Billy M Williams and Lester A Hoel. 2003. Modeling and forecasting vehicular traffic flow as a seasonal ARIMA process: Theoretical basis and empirical results. *Journal of transportation engineering* 129, 6 (2003), 664–672.
- [54] Xinle Wu, Dalin Zhang, Chenjuan Guo, Chaoyang He, Bin Yang, and Christian S. Jensen. 2021. AutoCTS: Automated Correlated Time Series Forecasting. *Proc. VLDB Endow.* 15, 4 (2021), 971–983.
- [55] Zonghan Wu, Shirui Pan, Guodong Long, Jing Jiang, Xiaojun Chang, and Chengqi Zhang. 2020. Connecting the dots: Multivariate time series forecasting with graph neural networks. In *KDD*. 753–763.
- [56] Z Wu, S Pan, G Long, J Jiang, and C Zhang. 2019. Graph WaveNet for Deep Spatial-Temporal Graph Modeling. In *IJCAI*. International Joint Conferences on Artificial Intelligence Organization.
- [57] Mingxing Xu, Wenrui Dai, Chunmiao Liu, Xing Gao, Weiyao Lin, Guo-Jun Qi, and Hongkai Xiong. 2020. Spatial-Temporal Transformer Networks for Traffic Flow Forecasting. *CoRR* abs/2001.02908 (2020).
- [58] Haoyang Yan, Xiaolei Ma, and Ziyuan Pu. 2022. Learning Dynamic and Hierarchical Traffic Spatiotemporal Features With Transformer. *IEEE Trans. Intell. Transp. Syst.* 23, 11 (2022), 22386–22399.
- [59] Huaxiu Yao, Xianfeng Tang, Hua Wei, Guanjie Zheng, and Zhenhui Li. 2019. Revisiting Spatial-Temporal Similarity: A Deep Learning Framework for Traffic Prediction. In *AAAI*. AAAI Press, 5668–5675.
- [60] Huaxiu Yao, Fei Wu, Jintao Ke, Xianfeng Tang, Yitian Jia, Siyu Lu, Pinghua Gong, Jieping Ye, and Zhenhui Li. 2018. Deep Multi-View Spatial-Temporal Network for Taxi Demand Prediction. In *AAAI*. AAAI Press, 2588–2595.
- [61] Junchen Ye, Zihan Liu, Bowen Du, Leilei Sun, Weimiao Li, Yanjie Fu, and Hui Xiong. 2022. Learning the Evolutionary and Multi-scale Graph Structure for Multivariate Time Series Forecasting. In *KDD*. ACM, 2296–2306.
- [62] Junchen Ye, Leilei Sun, Bowen Du, Yanjie Fu, and Hui Xiong. 2021. Coupled Layer-wise Graph Convolution for Transportation Demand Prediction. In *AAAI*. AAAI Press, 4617–4625.
- [63] Jiexia Ye, Juanjuan Zhao, Kejiang Ye, and Cheng-Zhong Xu. 2022. How to Build a Graph-Based Deep Learning Architecture in Traffic Domain: A Survey. *IEEE Trans. Intell. Transp. Syst.* 23, 5 (2022), 3904–3924.
- [64] Xue Ye, Shen Fang, Fang Sun, Chunxia Zhang, and Shiming Xiang. 2022. Meta Graph Transformer: A Novel Framework for Spatial-Temporal Traffic Prediction. *Neurocomputing* 491 (2022), 544–563.
- [65] Xueyan Yin, Genze Wu, Jinze Wei, Yanming Shen, Heng Qi, and Baocai Yin. 2021. Deep Learning on Traffic Prediction: Methods, Analysis and Future Directions. *IEEE Transactions on Intelligent Transportation Systems* (2021).
- [66] Bing Yu, Haoteng Yin, and Zhanxing Zhu. 2018. Spatio-temporal Graph Convolutional Networks: A Deep Learning Framework for Traffic Forecasting. In *Proceedings of the 27th International Joint Conference on Artificial Intelligence (IJCAI)*.
- [67] Jing Yuan, Yu Zheng, Xing Xie, and Guangzhong Sun. 2011. Driving with knowledge from the physical world. In *Proceedings of the 17th ACM SIGKDD international conference on Knowledge discovery and data mining*. 316–324.
- [68] Jing Yuan, Yu Zheng, Chengyang Zhang, Wenlei Xie, Xing Xie, Guangzhong Sun, and Yan Huang. 2010. T-drive: driving directions based on taxi trajectories. In *Proceedings of the 18th SIGSPATIAL International conference on advances in geographic information systems*. 99–108.
- [69] Hongyu Zang, Dongcheng Han, Xin Li, Zhifeng Wan, and Mingzhong Wang. 2022. CHA: Categorical Hierarchy-based Attention for Next POI Recommendation. *ACM Trans. Inf. Syst.* 40, 1 (2022), 7:1–7:22.
- [70] Jinlei Zhang, Feng Chen, Zhiyong Cui, Yinan Guo, and Yadi Zhu. 2020. Deep learning architecture for short-term passenger flow forecasting in urban rail transit. *IEEE Transactions on Intelligent Transportation Systems* (2020).
- [71] Jiani Zhang, Xingjian Shi, Junyuan Xie, Hao Ma, Irwin King, and Dit-Yan Yeung. 2018. GaAN: Gated Attention Networks for Learning on Large and Spatiotemporal Graphs. In *UAI*. AUAI Press, 339–349.
- [72] Junbo Zhang, Yu Zheng, and Dekang Qi. 2017. Deep spatio-temporal residual networks for citywide crowd flows prediction. In *Proceedings of the AAAI Conference on Artificial Intelligence*, Vol. 31.
- [73] Qi Zhang, Jianlong Chang, Gaofeng Meng, Shiming Xiang, and Chunhong Pan. 2020. Spatio-Temporal Graph Structure Learning for Traffic Forecasting. In *AAAI*. AAAI Press, 1177–1185.
- [74] Xiyue Zhang, Chao Huang, Yong Xu, Lianghao Xia, Peng Dai, Liefeng Bo, Junbo Zhang, and Yu Zheng. 2021. Traffic Flow Forecasting with Spatial-Temporal Graph Diffusion Network. In *AAAI*. AAAI Press, 15008–15015.
- [75] Ling Zhao, Yujiao Song, Chao Zhang, Yu Liu, Pu Wang, Tao Lin, Min Deng, and Haifeng Li. 2019. T-gcn: A temporal graph convolutional network for traffic prediction. *IEEE Transactions on Intelligent Transportation Systems* 21, 9 (2019), 3848–3858.
- [76] Chuanpan Zheng, Xiaoliang Fan, Cheng Wang, and Jianzhong Qi. 2020. GMAN: A Graph Multi-Attention Network for Traffic Prediction. In *AAAI*. AAAI Press, 1234–1241.
- [77] Ming Zhou, Jiarui Jin, Weinan Zhang, Zhiwei (Tony) Qin, Yan Jiao, Chenxi Wang, Guobin Wu, Yong Yu, and Jieping Ye. 2019. Multi-Agent Reinforcement Learning for Order-dispatching via Order-Vehicle Distribution Matching. In *CKM*. ACM, 2645–2653.
- [78] Xiao Wang, Peng Cui, Jing Wang, Jian Pei, Wenwu Zhu, and Shiqiang Yang. 2017. Community preserving network embedding. In *Proceedings of the AAAI conference on artificial intelligence*, Vol. 31.